ACCOUNTS
of chemical research

Charge-Transfer Excitons at Organic Semiconductor Surfaces and Interfaces

X.-Y. ZHU,* Q. YANG, AND M. MUNTWILER
Department of Chemistry, University of Minnesota, Minneapolis, Minnesota 55455

RECEIVED ON DECEMBER 17, 2008

CONSPECTUS

When a material of low dielectric constant is excited electronically from the absorption of a photon, the Coulomb attraction between the excited electron and the hole gives rise to an atomic H-like quasi-particle called an exciton. The bound electron−hole pair also forms across a material interface, such as the donor/acceptor interface in an organic heterojunction solar cell; the result is a charge-transfer (CT) exciton. On the basis of typical dielectric constants of organic semiconductors and the sizes of conjugated molecules, one can estimate that the binding energy of a CT exciton across a donor/acceptor interface is 1 order of magnitude greater than k_BT at room temperature (k_B is the Boltzmann constant and T is the temperature). *How can the electron−hole pair escape this Coulomb trap in a successful photovoltaic device?*

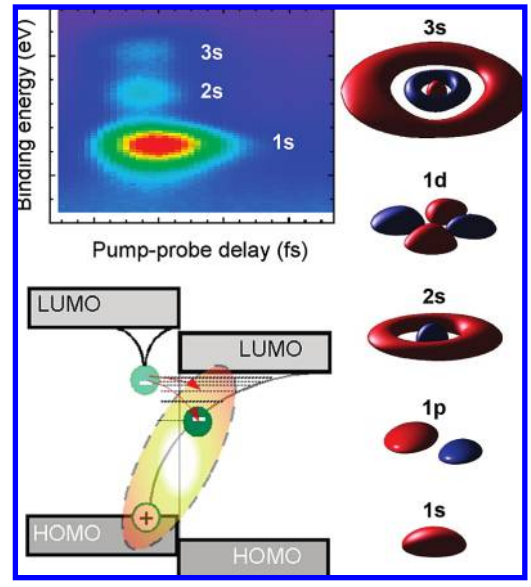

To answer this question, we use a crystalline pentacene thin film as a model system and the ubiquitous image band on the surface as the electron acceptor. We observe, in time-resolved two-photon photoemission, a series of CT excitons with binding energies ≤0.5 eV below the image band minimum. These CT excitons are essential solutions to the atomic H-like Schrödinger equation with cylindrical symmetry. They are characterized by principal and angular momentum quantum numbers. The binding energy of the lowest lying CT exciton with 1s character is more than 1 order of magnitude higher than k_BT at room temperature. The CT_{1s} exciton is essentially the so-called exciplex and has a very low probability of dissociation. We conclude that hot CT exciton states must be involved in charge separation in organic heterojunction solar cells because (1) in comparison to CT_{1s}, hot CT excitons are more weakly bound by the Coulomb potential and more easily dissociated, (2) density-of-states of these hot excitons increase with energy in the Coulomb potential, and (3) electronic coupling from a donor exciton to a hot CT exciton across the D/A interface can be higher than that to CT_{1s} as expected from energy resonance arguments. We suggest a design principle in organic heterojunction solar cells: there must be strong electronic coupling between molecular excitons in the donor and hot CT excitons across the D/A interface.

1. Fundamentals of Charge-Transfer Excitons

Excitons are atomic hydrogen-like bound electron−hole pairs that determine many optical and optoelectronic properties of solid materials.[1,2] If the radius of the electron−hole pair is smaller than the unit cell dimension, we call this a Frenkel or molecular exciton. If it is much larger than the unit cell size and the electron−hole pair possesses delocalized characteristics, we call this a Mott−Wannier exciton. A typical exciton consists of an electron and a hole located in the same spatial region and possesses no dipole moment. The situation is very different when there is an interface. The Coulombically bound electron and hole can be located in spatially separate regions across the

Published on the Web 04/20/2009 www.pubs.acs.org/acr
10.1021/ar800269u CCC: $71.50

interface. The result is a charge-transfer (CT) exciton possessing a dipole momentum.

Understanding CT excitons is essential to the development of excitonic solar cells. In a conventional p−n junction solar cell, the built-in potential separates the photoexcited electron and hole. In contrast, there may not be a built-in potential in an excitonic solar cell, and charge separation requires an energetic driving force provided by the differences in the electronic levels of the materials at the interface, i.e., a donor/acceptor (D/A) interface.[3−6] When the electron donor and/or acceptor are organic semiconductors,[7] the low dielectric constants ensure that charge separation at the D/A interface does not give free charge carriers but rather a bound electron−hole pair across the interface, i.e., a CT exciton. Two key questions arise: What is the binding energy of such a CT exciton? How is this binding energy overcome in a successful charge separation event to give photocurrent?

Consider a "toy" model of the CT exciton with a hole on the donor side and the electron on the acceptor side. An accurate treatment of this problem should take into account the translational symmetry of the donor and acceptor lattices as well as the spatial correlation of the electron and the hole. This presents a formidable theoretical challenge, as discussed in section 5. Here, we assume only the simplest possible scenario: a nearly free electron in the acceptor (e.g., in the conduction band) and a localized hole on a donor molecule or vice versa. Under these assumptions, the problem simply reduces to a single electron Hamiltonian for a hydrogenic atom of cylindrical symmetry

$$\hat{H} = -\frac{\hbar^2}{2\mu}\nabla^2 - \frac{e^2}{4\pi\varepsilon_0\varepsilon|\vec{r}_o + \vec{r}|} \qquad (1)$$

where μ is the reduced mass, ε is the dielectric constant, ε_0 is the vacuum permittivity, and r_o is the minimal electron−hole separation, e.g., the distance of the localized hole to the interface. We assume that (a) $\varepsilon = 3.15$ (a typical value for an organic semiconductor and equal to the average ε at the pentacene/vacuum interface; see below), (b) $r_o = 2.7$ Å (∼radius of an aromatic ring), (c) the electron is confined to half space (acceptor) with a hard wall at the interface, and (d) $\mu = m_e$ (a completely free electron and a completely localized hole). We solve the Schrödinger equation numerically using the finite element method within the COMSOL simulation software. The results, summarized in Figure 1, are a set of atomic hydrogen-like eigenfunctions with eigenvalues of $E \geq -0.2$ eV.

The above exercise suggests several important properties of CT excitons at organic semiconductor interfaces. First, there is not one but a series of CT excitons approaching the conduction band minimum. Second, the binding energy of the lowest lying CT exciton (1s) is 1 order of magnitude higher than k_BT at room temperature. Third, each CT exciton wave function possesses distinct symmetry, as governed by the principal quantum number (n) and the orbital angular momentum quantum number (l) in the z direction. Note that, because of cylindrical symmetry and the restriction of half space, the allowed angular momentum quantum number is not limited by the principal quantum number.

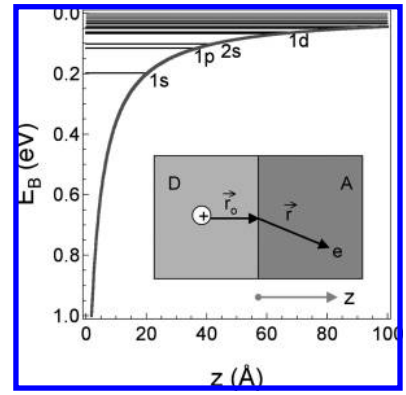

FIGURE 1. Eigenvalues for the CT exciton in the H-atom model. The potential shown is along z. The binding energy (E_B) is referenced to the conduction band minimum.

2. Experimental Observation of CT Excitons

The toy model presented above for CT excitons has been realized in recent experiments in our laboratory.[8,9] We probe CT excitons on crystalline organic semiconductor surfaces using time-resolved two-photon photoemission (TR-2PPE) spectroscopy. We use vapor-deposited crystalline pentacene thin films grown on either the semi-metal Bi(111) surface or the Si(111) surface in an ultrahigh vacuum environment. Pentacene thin films of bulk crystalline structure, with the long molecular axis nearly perpendicular to the substrate surface, are known to grow epitaxially on the Bi(111) surface.[10] On the Si surface, besides the chemisorbed and lying-down wetting layer, polycrystalline pentacene thin films of bulk-like structure grow beyond the first layer.[11] For an electron above the surface of a polarizable medium, e.g., the pentacene thin film, there are two types of transient states (Figure 2): the delocalized image potential state (IPS) and the localized CT exciton state. An electron on the surface of a polarizable material is attracted to the surface because of the interaction between the electron and oppositely charged polarization distribution; the net result is equivalent to the Coulomb interaction between the electron and a fictitious positive image charge located below the surface (hence, the name of the image potential state). The elec-

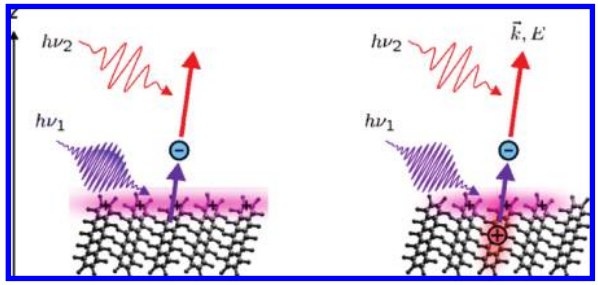

FIGURE 2. Probing image potential states (left) and CT excitons (right) on an organic semiconductor surface by TR-2PPE.

tron is localized in the *z* direction by the image potential but is delocalized in the *xy* plane. When a real hole is also present at the surface (localized to an organic molecule), the electron is then bound by both the image potential and the electron−hole Coulomb potential.

In a TR-2PPE experiment,[12] two femtosecond laser pulses (with photon energy typically below the workfunction) are focused onto the sample surface and the resulting photoelectron because of two-photon excitation is detected in an electron energy analyzer. In the present experiment, the first photon ($h\nu_1$) excites an electron from the highest occupied molecular orbital (HOMO) to the CT exciton state above the surface. After a controlled time delay, the second photon ($h\nu_2$) excites the transiently bound electron to above the vacuum level for detection. When carried out in the angle-resolved mode, TR-2PPE also measures the parallel momentum vector and, thus, band dispersion.

The pseudo-color plots in Figure 3 show TR-2PPE spectra taken at different pump−probe time delays from monolayer (ML) pentacene/Bi(111) (lower) and multilayer pentacene (>10 nm) on Si(111) (upper). One can identify at least three CT exciton states below the $n = 1$ image potential state. Note that the peaks are better resolved on the highly crystalline ML pentacene/Bi(111) surface than on the polycrystalline multilayer pentacene/Si(111) surface. The distinction between the IPS and the CT exciton states is established in angle-resolved measurements: the IPS shows free electron-like parallel dispersion (i.e., *energy* versus parallel momentum vector), which can be fit with an effective mass of $m_{\text{eff}} = 1.5m_e$, while the CT exciton states show no parallel dispersion.[8] With reference to the bottom of the image band, the three CT excitons on the ML pentacene/Bi(111) surface are bound by energies of 0.44, 0.24, and 0.08 eV, respectively. On the multilayer pentacene/Si(111) surfaces, the binding energies of the three CT states are 0.52, 0.30, and 0.09 eV. On the basis of quantum mechanical modeling, we assign these three states to the 1s, 2s, and 3s CT excitons, respectively, as detailed below.

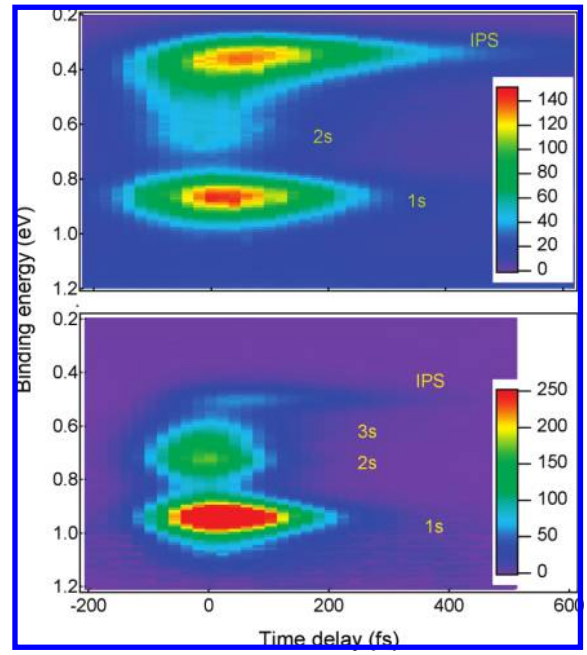

FIGURE 3. Pseudo-color plots of TR-2PPE spectra at different pump−probe delay times for 1 ML pentacene/Bi(111) (lower, $h\nu_1 = 4.38$ eV) and multilayer pentacene/Si(111) (upper, $h\nu_2 = 4.77$ eV). Each vertical cut corresponds to an electron energy-resolved 2PPE spectrum at a particular pump−probe delay. The color scale is photoelectron intensity (10^3 counts/s). The binding energy scale is referenced to the vacuum level.

In molecular photophysics, it is well-known that when high-energy singlet states are excited, they often quickly relax to the lowest energy singlet state. This is also observed for CT excitons on the pentacene surface. Figure 4 shows cross-correlation (CC) curves for various states probed at two photon energies for 1 ML pentacene/Bi(111). Each curve corresponds to photoelectron intensity at a particular electron energy recorded as a function of pump−probe delay. At $h\nu_1 = 4.17$ eV, which is in resonance with the HOMO → CT_{1s} transition, only the CT_{1s} state is excited. Fitting the CC curve to a simple rate equation model shows that CT_{1s} is populated directly by $h\nu_1$ without any time delay ($t_0 = 0$) and decays with a time constant of $\tau = 56$ fs. The IPS (delayed by $t_0 = 44$ fs) is populated indirectly by photoexcitation in the Bi substrate followed by electron transfer through the pentacene film to the image potential state. When $h\nu_1$ is increased to 4.38 eV, CT excitons above CT_{3s} are resonantly excited. The highly excited states relaxes down the CT exciton manifold, as evidenced by the sequential increase in the delay time of populating lower lying states ($t_0 = 19$, 35, and 51 fs for 3s, 2s, and 1s, respectively).

Note that the CT excitons observed on pentacene surfaces are short-lived (lifetime < 100 fs). This is because at the organic−vacuum interface the CT excitons are referenced to

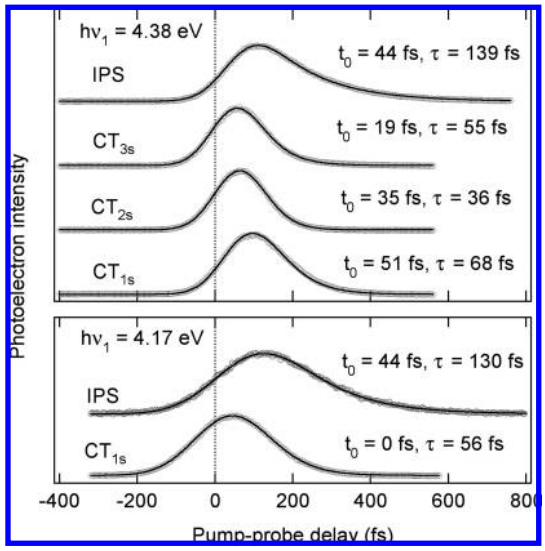

FIGURE 4. Two-photon photoemission cross-correlation curves of the CT excitons and the IPS on 1 ML pentacene/Bi(111) measured at $h\nu_1 = 4.17$ eV (lower) and 3.38 eV (upper). We determine the transient state lifetimes by fitting to the rate equation model using a Gaussian pulse profile. t_0 is the temporal offset of the Gaussian with respect to zero pump−probe delay. Dots represent raw data, and solid lines are fits. The curves are normalized and vertically offset for clarity.

the image band, which lies high in energy, well above the band gaps of the organic semiconductors. As a result, the CT excitons can resonantly decay into highly excited molecular excitons within the organic semiconductor, resulting in short lifetimes. In contrast, CT excitons formed at a D/A interface in an organic photovoltaic device are energetically located in the band gap of either the donor or the acceptor. These CT excitons are much longer lived.

To aid the assignment of IPS and CT exciton states on the pentacene surface, we carry out numerical simulation within the dielectric continuum approximation. In the simplistic model presented above, we assumed a localized hole on the donor side and a free electron on the acceptor side. This simplification is justified for CT excitons on a pentacene surface because (a) the image band, i.e., the acceptor, is free electron-like and (b) the HOMO band of pentacene or tetracene is nearly flat near the Γ point,[13,14] corresponding to heavy effective hole mass. However, unlike a more realistic organic D/A system, where the dielectric constant is not expected to change much across the interface, there is a dramatic change in dielectric constant from that of the organic semiconductor to that of vacuum ($\varepsilon_{vac} = 1$). This difference in dielectric constants introduces an additional potential, the image potential (last term),[15] to the Hamiltonian

$$\hat{H} = -\frac{\hbar^2}{2\mu}\nabla^2 - \frac{e^2\gamma}{4\pi\varepsilon_0|\vec{r}_0 + \vec{r}|} - \frac{e^2}{4\pi\varepsilon_0}\frac{\beta}{4z} \qquad (2)$$

where z is the distance of the electron to the interface (the image plane) and $\beta = (\varepsilon - 1)/(\varepsilon + 1)$ and $\gamma = 2/(\varepsilon + 1)$ account for screening of the charge because of the polarizability of pentacene ($\varepsilon = 5.3$). Note that $1/\gamma$ (=3.15) is the average dielectric constant used in simulating the results in Figure 1.

A typical set of simulation results is shown in Figure 5. The eigenvalues can be divided into two regimes: a band of delocalized states, which corresponds to the image band, and a series of localized, bound states converging toward the bottom of the image band. The eigenfunctions of the localized states are very similar to those in the toy model in Figure 1. These are the CT excitons. For multilayer pentacene, the binding energies of the three CT exciton states observed in 2PPE spectra (BE = 0.52, 0.30, and 0.09 eV) are in good agreement with those of the 1s, 2s, and 3s states in simulation based on a r_0 value of 2.7 Å. This r_0 value corresponds to a hole localized mainly in the aromatic ring nearest the surface. The simulation predicts that the 1p state is located between 1s and 2s; however, this state is missing in the experiment spectra (Figure 3). The photoemission selection rule dictates that cross-sections from states with in-plane nodes are null in photoemission in the surface normal direction.[16] Other allowed transitions are not resolved because of spectral congestion.

Note that, when referenced to the bottom of the image band, the CT exciton binding energies in Figure 5 are nearly twice the corresponding values in Figure 1. This is because the presence of the image contribution makes the total potential much steeper in the z direction. The steeper potential is also reflected in $\langle r \rangle$, which decreases from ~13 Å in Figure 1 to

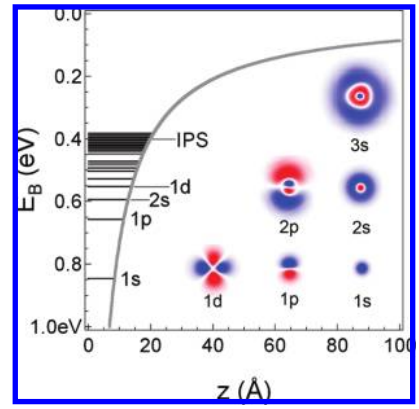

FIGURE 5. Eigenvalues and eigenfunctions (the first six) obtained from the dielectric continuum model for CT excitons on the surface. The potential shown is along the direction normal to the surface. The bottom of the image potential band is labeled with IPS.

~7 Å in Figure 5. A correction must be made to account for the image potential contribution when one infers the CT exciton binding from the model systems studied above for real D/A interfaces. Strictly speaking, the e−h Coulomb potential is not separable from the image potential. Thus, referencing the CT excitons to the bottom of the image band is an approximation.

3. Generality of CT Excitons on Surfaces: A Prediction

What determines the formation of a CT exciton on a solid surface? The criteria seem very simple: a hole must be localized to the surface region without complete screening by the dielectric response of the material. This means most nonmetal solids. Image potential states or resonances can exist on all polarizable surfaces (particularly metal surfaces) because of the universal nature of the image potential. Similarly, we predict that CT excitons should be of general significance to nonmetal surfaces, given the ubiquitous nature of the Coulomb potentials in eqs 1 and 2. The key is localization of the hole to the surface region. This is a common situation in molecular semiconductors with relatively narrow valence bandwidth.

When hole delocalization in the HOMO band becomes significant, the CT exciton should adopt some delocalized band-like Mott−Wannier characteristics. The crystalline structures of molecular solids are typically anisotropic. For example, pentacene or tetracene is a layered solid, with the long molecular axis nearly perpendicular to the plane of the herringbone-packed molecular layer. Band dispersion is significant in the molecular plane but negligible in the perpendicular direction. Thus, these CT excitons should possess some Mott−Wannier characteristics, i.e., delocalization in the surface plane. We hypothesize that possessing Mott−Wannier characteristics may be important for the experimental observation of surface CT excitons in 2PPE spectroscopy. These CT excitons are mixed with the image states that delocalize in the surface plane. The optical transition dipole moment is enhanced when the initial state (HOMO band) is also delocalized in the same spatial region (surface plane). In comparison, the transition dipole moment is negligible between localized and delocalized states. In partial support of this hypothesis, we fail to observe CT excitons on the surface of less crystalline organic semiconductor thin films, including rubrene vapor deposited on Si(111) or pentacene vapor deposited at cryogenic temperatures. At a realistic D/A interface with significant disorder, both the initial HOMO state in the donor and the CT exciton state across the interface can be localized and direct optical excitation is also possible.[17]

Delocalization of excitons in organic semiconductors has been reported before. Forrest and co-workers demonstrated a quantum confinement effect on Wannier-type excitons in crystalline organic semiconductor thin films (quantum wells).[18−20] Lim et al. reported exciton delocalization in crystalline tetracene.[21] Schuster et al. directly measured the exciton band structure of crystalline pentacene and showed a bandwidth of ~10 meV.[22] For an interfacial CT exciton probed here, even if it may possess significant Mott−Wannier characteristics, dispersion of the CT exciton band cannot be observed in a photoemission experiment. This is because the photoemission process destroys the exciton (quasi-particle). A simplistic view of this problem is that the hole left behind can carry away with an undetermined amount of momentum. A viable technique to map out CT exciton dispersion is inelastic electron scattering.[22]

4. Hot CT Exciton Mechanism in Organic Photovoltaics

The pentacene/vacuum interface represents a simplistic model for donor/acceptor interfaces in organic photovoltaics because the electron−hole attraction potential in the former system is equivalent to that at a D/A interface, with an average dielectric constant of $\varepsilon = 3.15$, a typical value for organic or polymeric semiconductors. It is usually believed that the electrostatic attraction at a D/A interface is on the order of ~0.5 eV. This is estimated from the Coulomb potential based on an e−h distance of 1 nm and a dielectric constant of $\varepsilon \sim 3$. Now, we come back to the question posed earlier: *How is this binding energy overcome in a successful charge separation event to give photocurrent?*

The CT_{1s} exciton binding energy is 1 order of magnitude higher than k_BT at room temperature. On the basis of thermodynamic arguments, the probability of charge separation from such an e−h pair is proportional to $\exp(-E_B/k_BT)$ and is, thus, small. The entropic driving force favors charge carrier separation and carrier diffusion away from the interface,[23] but this alone is insufficient to give a high charge separation efficiency. Thus, the fate of the CT_{1s} exciton is likely charge recombination. In fact, the CT_{1s} exciton is essentially what is called the exciplex in previous studies.[24−26] The only difference lies in the extent of reorganization in the nuclear coordinates (bath); the exciplex can be considered a self-trapped CT_{1s} exciton (i.e, a polaron−exciton). An exciplex can be formed at D/A interfaces from the dissociation of a photoexcited Frenkel exciton

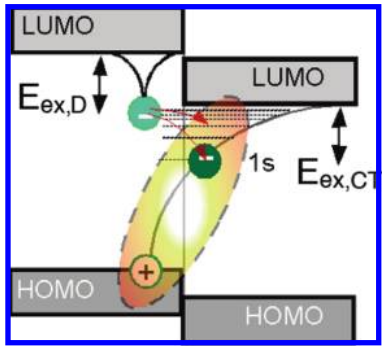

FIGURE 6. Dissociation of an exciton in the donor to form the 1s or hot CT excitons across the D/A interfaces.

in the donor or acceptor,[24−26] from an electron and a hole injected electrically in a diode geometry,[27] or from direct below-gap optical excitation in a D/A blend.[17]

We believe that efficient charge separation at an organic D/A interface must involve hot CT exciton states, as shown schematically in Figure 6. Before proceeding further, we would like to clarify a common misconception in drawing energy level diagrams. Consider the single-particle energy level diagram in Figure 6. Here, the HOMO and lowest unoccupied molecular orbital (LUMO) levels are transport levels, each corresponding to the energy of an excess hole in the HOMO or an excess electron in the LUMO. An exciton is a quasi-particle, and its energy is referenced internally. In principle, an exciton *cannot* be represented on such a single electron diagram. In practice, we are willing to sacrifice physical accuracy for convenience. One common practice is to equally divide the exciton binding energy and represent the exciton as consisting of two interacting single particle levels, with the "electron" at $0.5E_{ex}$ below the conduction band minimum (CBM) and the hole at $0.5E_{ex}$ above the valence band maximum (VBM). For the purpose of this Account, we prefer to associate the exciton binding energy with one of the fictitious single particle levels. For electron transfer in Figure 6, we associate the exciton binding energy entirely with the electron; after *complete* exciton dissociation, the hole adopts the transport level associated with the HOMO, while the electron is associated with the LUMO. This picture allows one to easily visualize the energetic driving force as the difference in LUMO levels between the donor and the acceptor. Similarly, for hole transfer, a convenient picture is to associate the acceptor exciton binding energy entirely with the hole level.

Accepting the "inaccurate" cartoon in Figure 6, we can now come back to the charge separation problem at organic D/A interfaces. There is a minimum energy requirement: the energetic driving force, Δ_{LUMO} (difference in LUMO levels between the donor and acceptor), needs to be larger than the binding energy of the exciton in the donor, $E_{ex,D}$. If this requirement is satisfied, decaying from an exciton in the donor to any CT exciton across the D/A interface is a downhill process. As discussed above, if the CT_{1s} exciton is formed, the consequence, in the absence of a strong electric field, is likely radiative charge recombination. The probability for charge separation is much higher when the intermediates are hot CT excitons because of their lower binding energies. We can identify several factors that may influence hot CT exciton formation and free carrier generation as follows:

The first factor is the excess energy released when an exciton in the donor decays to the CT exciton at the interface. Within the classic Onsager picture for ion-pair separation,[28,29] we can view such excess energy as kinetic energy, which assists the electron and/or hole in escaping from the Coulomb potential. Quantum mechanically, the excess energy favors the formation of CT exciton states with high internal quantum numbers and/or high k states when some delocalization, i.e., Mott−Wannier character, is present.

The second factor is the extent of delocalization. Crystallinity of the organic semiconductor can lead to high carrier mobility (at least locally within the crystalline domain). A higher carrier mobility, particularly more disparity in the mobilities between the two carriers,[30] increases the probability for the two carriers to escape from each other. Quantum mechanically, increased crystallinity gives more delocalized contribution to the total wave function; delocalization favors charge separation.

The third factor is electronic coupling between the exciton in the donor and CT excitons across the interface. The strength of electronic coupling is determined by the detailed shapes of the wave functions, e.g., spatial extent and symmetry, for both types of excitons involved.[31,32] Hotter CT excitons are energetically more resonant with the donor exciton, and this can, in principle, lead to stronger electronic coupling because of lower energy denominators. The density-of-states of hot CT excitons increases with energy in the Coulomb potential, which may also increase their coupling to the donor exciton.

The fourth factor is local electric fields. An electric field favoring charge separation may come from unintentional doping,[33] which leads to interfacial charge redistribution resembling a conventional p/n junction.[34] Alternatively, an interfacial field may come from charge redistribution or polarization at the D/A interface, as predicted by Kahn and co-workers based on the concept of the charge neutrality level.[35] Arkhipov, Heremans, and Bässler explained efficient charge separation based on such a dipole layer at the D/A interface.[36] The field

at the D/A interfaces has been measured by Asbury and co-workers based on a vibrational Stark effect.[37]

Other factors, such as charge carrier trapping and intermediate energy levels, also contribute to exciton dissociation. Trapping of one charge species, e.g., to an impurity site, may facilitate dissociation of a CT exciton but without contribution to the photocurrent. The presence of intermediate energy levels (stepping stones) at the interface because of different molecular structures (e.g., crystalline versus amorphous) or intentionally added interfacial molecules may also facility hot CT exciton formation and charge separation.[38,39] This last factor is well-known in the photosynthetic system, where nature has developed an assembly of molecules to efficiently transfer the photoexciton energy from a chromophore through a cascade to the reaction center.[40]

The proposal of hot CT excitons as responsible for photocurrent generation in organic solar cells is not new. Similar ideas have been put forward within the classical framework of Onsager's theory for ion-pair separation.[28,29] Three decades ago, Yokoyama et al.[41−43] studied extrinsic carrier generation in poly-*N*-vinylcarbazole doped with weak electron acceptors. They interpreted the partial quenching of exciplex fluorescence by an applied electric field as a result of the initial formation of a nonrelaxed exciplex state, which could either relax to the emissive exciplex state or thermally dissociate (with assistance from the applied field) to free carriers. Yokoyama et al. estimated that the electron−hole distance in the nonrelaxed exciplex state was 22 Å. Morteani et al. measured charge separation efficiency as a function of the external bias voltage for a D/A blend and suggested that charge separation came not from the exciplex but from long distance geminate pairs, with e−h separation of 22−31 Å.[44] The long distance geminate pair can relax to the exciplex and then endothermically back to the donor exciton (back electron transfer). Blom and co-workers explained the temperature and electric field dependences of photocurrent generation in polymer−fullerene bulk heterojunctions by assuming a distribution of initial e−h separations with a mean at $\langle r \rangle = 15$ Å.[45] Peumans and Forrest carried out Monte Carlo simulation for charge carrier separation at D/A interfaces and found that, for an initial e−h distance of 40 Å, the geminate pair dissociation probability is only 0.1 in the absence of field.[30] Note that the classical picture of a long-distance or nonrelaxed geminate pair is essentially a hot CT exciton (or a superposition of hot CT excitons) in the quantum mechanical picture.

The binding energy of a geminate pair or CT exciton across a D/A interface is a sensitive function of the e−h distance and, thus, the structural parameters involved. Recently, Schmidtke, Friend, and Silva illustrated this simple argument in an elegant experiment using a polymer D/A blend under hydrostatic pressure.[46] Fluorescence from the exciplex red shifts by 270−370 meV when the pressure is increased from 0.1 MPa to 8.8 GPa. The authors argued that exciplex emission is favored over charge separation at high pressures because of the increased CT exciton binding energy.

5. Spatial Correlation and Delocalization: Challenges to Theory

The model systems and discussions presented above deal with the simplest type of CT excitons, namely, a free electron in the acceptor interacting with a localized hole in the donor (or vice versa). This may approximate the situation when one of the materials across the D/A interface possesses significant crystallinity and band dispersion.[47] However, a real D/A interface can deviate substantially from the "toy" model in Figure 1. We can identify two extremes and the possibilities in between.

One extreme involves a completely localized donor interacting with a completely localized acceptor. Both experiments and theories are well-developed for this kind of localized charge transfer and separation,[48] particularly in the extensively explored system of donor−acceptor (D−A) or donor−bridge−acceptor (D−B−A) molecules.[49,50] In a D−A or D−B−A molecule, initial photoexcitation occurs in the donor group; this is followed by electron transfer and charge separation. There have been extensive theoretical investigations of these localized charge separation processes. In the weak electronic coupling region, the rate of charge separation can be described by Fermi's golden rule and is determined by three key parameters: electronic coupling, free-energy change, and reorganization energy. These microscopic parameters can be calculated from conventional quantum chemical methods. More advanced theoretical approaches go beyond the single electron description and may use configuration interaction (CI) to properly treat the excited states.[48] Here, the CT exciton state is one of the excited states, in particular, $\Psi_{CT}(D^+A^-)$. These quantum chemical methods have been used recently to model localized charge separation at van der Waals D/A interfaces of interest in organic or polymeric photovoltaics.[31,32]

The other extreme involves a delocalized donor and a delocalized acceptor (e.g., crystalline D/A interfaces). On the one hand, both the electron and hole are located in delocalized bands with translational symmetry and are thus represented by momentum vectors ($\boldsymbol{k}_A$ for an electron in the acceptor LUMO or conduction band and $\boldsymbol{k}_D$ for a hole in the

donor HOMO or valence band); the momentum vector of the CT exciton is thus $\boldsymbol{K} = \boldsymbol{k}_A - \boldsymbol{k}_D$. On the other hand, the spatial correlation of the electron and the hole across the D/A interface because of the Coulomb potential necessitates the introduction of a spatial vector $\boldsymbol{\beta}$, which represents the relative position of the electron to that of the hole. The total wave function of the CT exciton, $\Psi_{CT}(\boldsymbol{K}, \boldsymbol{\beta})$, takes into account both delocalization and spatial correlation but is very challenging to solve from a theoretical perspective.[1,2,47] Adding to this difficulty is the need to include electron−nuclear coupling to form self-trapped excitons. This has been performed in continuum models by Toyozawa and others, but there is little success on including atomic/molecular details.

In the case of organic or polymeric D/A interfaces, models from both extremes are likely not sufficient. There is experimental evidence that some extent of crystallinity of the donor and/or acceptor phase may facilitate charge separation, e.g., in the well-known case of the P3HT/PCBM system. As discussed earlier, delocalization can lead to high carrier mobility and an increase in the probability for the two carriers to escape from each other. How one incorporates delocalization in the traditional molecular CT models is, in our view, a key theoretical/computational challenge in developing a quantitative understanding of organic photovoltaics.

This work was supported by the National Science Foundation under award number DMR-0804583. Partial support from the MRSEC Program of the National Science Foundation under award number DMR-0819885 is also acknowledged.

BIOGRAPHICAL INFORMATION

Xiaoyang Zhu is the Merck Professor of Chemistry at the University of Minnesota. He received his Ph.D. from the University of Texas at Austin in 1989. After postdoctoral research with J. Mike White at University of Texas (UT)—Austin and Gerhard Ertl at the Fritz-Haber-Institute, he joined the faculty at Southern Illinois University as an Assistant Professor in 1993. In 1997, he moved to the University of Minnesota as an Associate Professor and later a Full Professor of Chemistry. Zhu directs and conducts research in two areas: (1) interfacial electron transfer in solar cells and organic electronics and (2) chemistry and physics of soft interfaces. His honors include a Dreyfus New Faculty Award, a Cottrell Scholar Award, and a Friedrich Wilhelm Bessel Award. Zhu is returning to his alma mater as the Louis Nicolas Vauquelin Regents Professor of Chemistry at UT—Austin.

Qingxin Yang was born in China in 1973. He received his Ph.D. in physics from Jilin University in 2000 and currently works as a research associate in the group of X.-Y. Zhu at the University of Minnesota. His interests include ultrafast exciton dynamics and nonlinear optical spectroscopy of organic semiconductors.

Matthias Muntwiler received his Ph.D. in experimental physics in 2004 from the University of Zurich, Switzerland, under the supervision of Prof. Jürg Osterwalder. In 2004, he joined the group of X.-Y. Zhu at the University of Minnesota as a research associate. His research focuses on electronic interactions at interfaces of small organic molecules and inorganic substrates, in particular, the dynamics of excited states in organic semiconductors. He is returning to Switzerland to join the Paul Scherrer Institute.

FOOTNOTES

*To whom correspondence should be addressed. E-mail: zhu@umn.edu.

REFERENCES

1 Toyozawa, Y. *Optical Processes in Solids*; Cambridge University Press: Cambridge, U.K., 2003.
2 Song, K. S.; Williams, R. T. *Self-Trapped Excitons*; Springer: Berlin, Germany, 1996.
3 Arkhipov, V. I.; Bässler, H. Exciton dissociation and charge photogeneration in pristine and doped conjugated polymrs. *Phys. Status Solidi A* **2004**, *201*, 1152–1187.
4 Rand, B. P.; Burk, D. P.; Forrest, S. R. Offset energies at organic semiconductor heterojunctions and their influence on the open-circuit voltage of thin-film solar cells. *Phys. Rev. B: Condens. Matter Mater. Phys.* **2007**, *75*, 115327.
5 Scharber, M.; Mühlbacher, D.; Koppe, M.; Denk, P.; Waldauf, C.; Heeger, A.; Brabec, C. Design rules for donors in bulk-heterojunction solar cells—Towards 10 % energy-conversion efficiency. *Adv. Mater.* **2006**, *18*, 789–794.
6 Ohkita, H.; Cook, S.; Astuti, Y.; Duffy, W.; Tierney, S.; Zhang, W.; Heeney, M.; McCulloch, I.; Nelson, J.; Bradley, D. D. C.; Durrant, J. R. Charge carrier formation in polythiophene/fullerene blend films studied by transient absorption spectroscopy. *J. Am. Chem. Soc.* **2008**, *130*, 3030–3042.
7 Silinsh, E. A.; Capek, V. *Organic Molecular Crystals: Interaction, Localization, and Transport Phenomena*; AIP Press: Woodbury, NY, 1994.
8 Muntwiler, M.; Yang, Q.; Tisdale, W. A.; Zhu, X.-Y. Coulomb barrier for charge separation at an organic semiconductor interface. *Phys. Rev. Lett.* **2008**, *101*, 196403.
9 Yang, Q.; Muntwiler, M.; Zhu, X.-Y. Charge transfer excitons and image potential states on pentacene and tetracene surfaces. Manuscript to be published.
10 Sadowski, J. T.; Nagao, T.; Yaginuma, S.; Fujikawa, Y.; Al-Mahboob, A.; Nakajima, K.; Sakurai, T.; Thayer, G. E.; Tromp, R. M. Thin bismuth film as a template for pentacene growth. *Appl. Phys. Lett.* **2005**, *86*, 073109.
11 Meyer zu Heringdorf, F.-J.; Reuter, M. C.; Tromp, R. M. Growth dynamics of pentacene thin films. *Nature* **2001**, *412*, 517–520.
12 Lindstrom, C.; Zhu, X.-Y. Photoinduced electron transfer at molecule−metal interfaces. *Chem. Rev.* **2006**, *106*, 4281–4300.
13 Hummer, K.; Ambrosch-Draxl, C. Electronic properties of oligoacenes from first principles. *Phys. Rev. B: Condens. Matter Mater. Phys.* **2005**, *72*, 205205.
14 Kakuta, H.; Hirahara, T.; Matsuda, I.; Nagao, T.; Hasegawa, S.; Ueno, N.; Sakamoto, K. Electronic structures of the highest occupied molecular orbital bands of a pentacene ultrathin film. *Phys. Rev. Lett.* **2007**, *98*, 247601.
15 Cole, M. W. Electronic surface states of a dielectric film on a metal substrate. *Phys. Rev. B: Condens. Matter Mater. Phys.* **1971**, *3*, 4418–4422.
16 Hufner, S. *Photoelectron Spectroscopy: Principles and Applications*, 3rd ed.; Springer-Verlag: Berlin, Germany, 2003.
17 Hallermann, M.; Haneder, S.; Da Como, E. Charge-transfer states in conjugated polymer/fullerene blends: Below-gap weakly bound excitons for polymer photovoltaics. *Appl. Phys. Lett.* **2008**, *93*, 053307.
18 So, F. F.; Forest, S. R. Evidence for exciton confinement in crystalline organic multiple quantum wells. *Phys. Rev. Lett.* **1991**, *66*, 2649–2652.
19 Haskal, E. I.; Shen, Z.; Burrows, P. E.; Forrest, S. R. Excitons and exciton confinement in crystalline organic thin films grown by organic molecular-beam deposition. *Phys. Rev. B: Condens. Matter Mater. Phys.* **1995**, *51*, 4449–4462.
20 Shen, Z.; Forrest, S. R. Quantum size effects of charge-transfer excitons in nonpolar molecular organic thin films. *Phys. Rev. B: Condens. Matter Mater. Phys.* **1997**, *55*, 10578–10592.
21 Lim, S.-H.; Bjorklund, T. G.; Spano, F. C.; Bardeen, C. J. Exciton delocalization and superradiance in tetracene thin films and nanoaggregates. *Phys. Rev. Lett.* **2004**, *92*, 107402.
22 Schuster, R.; Knupfer, M.; Berger, H. Exciton band structure of pentacene molecular solids: Breakdown of the Frenkel exciton model. *Phys. Rev. Lett.* **2007**, *98*, 037402.

23 Gregg, B. A. The photoconversion mechanism of excitonic solar cells. *MRS Bull.* **2005**, *31* (1), 20.

24 Halls, J. J. M.; Cornil, J.; dos Santos, D. A.; Silbey, R.; Hwang, D. H.; Holmes, A. B.; Brédas, J. L.; Friend, R. H. Charge- and energy-transfer processes at polymer/polymer interfaces: A joint experimental and theoretical study. *Phys. Rev. B: Condens. Matter Mater. Phys.* **1999**, *60*, 5721–5727.

25 Morteani, A. C.; Dhoot, A. S.; Kim, J.-S.; Silva, C.; Greenham, N. C.; Murphy, C.; Moons, E.; Ciná, S.; Burroughes, J. H.; Friend, R. H. Barrier-free electron-hole capture in polymer blend heterojunction light-emitting diodes. *Adv. Mater.* **2003**, *15*, 1708–1712.

26 Müller, J. G.; Lupton, J. M.; Feldmann, J.; Lemmer, U.; Scharber, M. C.; Sariciftci, N. S.; Brabec, C. J.; Scherf, U. Ultrafast dynamics of charge carrier photogeneration and geminate recombination in conjugated polymer:fullerene solar cells. *Phys. Rev. B: Condens. Matter Mater. Phys.* **2005**, *72*, 195208.

27 Cao, Y.; Parker, I. D.; Yu, G.; Zhang, C.; Heeger, A. J. Improved quantum efficiency for electroluminescence in semiconducting polymers. *Nature* **1999**, *397*, 414–417.

28 Onsager, L. Initial recombination of ion pairs. *Phys. Rev.* **1938**, *54*, 554–557.

29 Scher, H.; Rackovsky, S. Theory of geminate recombination on a lattice. *J. Chem. Phys.* **1984**, *81*, 1994–2009.

30 Peumans, P.; Forrest, S. R. Separation of geminate charge-pairs at donor—acceptor interfaces in disordered solids. *Chem. Phys. Lett.* **2004**, *398*, 27–31.

31 Kawatsu, T.; Coropceanu, V.; Ye, A.; Brédas, J.-C. Quantum-chemical approach to electronic coupling: Application to charge separation and charge recombination pathways in a model molecular donor—acceptor system for organic solar cells. *J. Phys. Chem. C* **2008**, *112*, 3429–3433.

32 Huang, Y.-S.; Westenhoff, S.; Avilov, I.; Sreearunothai, P.; Hodgkiss, J. M.; Deleener, C.; Friend, R. H.; Beljonne, D. Electronic structures of interfacial states formed at polymeric semiconductor heterojunctions. *Nat. Mater.* **2008**, *7*, 483–489.

33 Liu, A.; Zhao, S.; Rim, S.-B.; Wu, J.; Könemann, M.; Erk, P.; Peumans, P. Control of electric field strength and orientation at the donor—acceptor interface in organic solar cells. *Adv. Mater.* **2008**, *20*, 1065–1070.

34 Kahn, A.; Zhao, W.; Gao, W.; Vazquez, H.; Flores, F. Doping-induced realignment of molecular levels at organic—organic heterojunctions. *Chem. Phys.* **2006**, *325*, 129–137.

35 Vazquez, H.; Gao, W.; Flores, F.; Kahn, A. Energy level alignment at organic heterojunctions: Role of the charge neutrality level. *Phys. Rev. B: Condens. Matter Mater. Phys.* **2005**, *71*, 041306R.

36 Arkhipov, V. I.; Heremans, P.; Bässler, H. Why is exciton dissociation so efficient at the interface between a conjugated polymer and an electron acceptor? *Appl. Phys. Lett.* **2003**, *82*, 4605–4607.

37 Barbour, L. W.; Hegadorn, M.; Asbury, J. B. Watching electrons move in real time: Ultrafast infrared spectroscopy of a polymer blend photovoltaic material. *J. Am. Chem. Soc.* **2007**, *129*, 15884–15894.

38 Sista, S.; Yao, Y.; Yang, Y.; Tang, M. L.; Bao, Z. Enhancement in open circuit voltage through a cascade-type energy band structure. *Appl. Phys. Lett.* **2007**, *91*, 223508.

39 Ravirajan, P.; Peiró, A. M.; Nazeeruddin, M. K.; Graetzel, M.; Bradley, D. D. C.; Durrant, J. R.; Nelson, J. Hybrid polymer/zinc oxide photovoltaic devices with vertically oriented ZnO nanorods and an amphiphilic molecular interface layer. *J. Phys. Chem. B* **2006**, *100*, 7635–7639.

40 Gust, D.; Moore, T. A.; Moore, A. L. Mimicking photosynthetic solar energy transduction. *Acc. Chem. Res.* **2001**, *34*, 40–48.

41 Yokoyama, M.; Endo, Y.; Mikawa, H. Quenching of exciplex fluorescence by an electric field in the solid state. *Chem. Phys. Lett.* **1975**, *34*, 597–600.

42 Yokoyama, M.; Endo, Y.; Mikawa, H. Extrinsic carrier photogeneration in poly(*N*-vinylcarbazole) films doped with dimethyl terephthalate. *Bull. Chem. Soc. Jpn.* **1976**, *49*, 1538–1541.

43 Yokoyama, M.; Endo, Y.; Matsubara, A.; Mikawa, H. Mechanism of extrinsic carrier generation in poly-*N*-vinylcarbazole. II. Quenching of exciplex fluorescence by electric field. *J. Chem. Phys.* **1981**, *75*, 3006–3011.

44 Morteani, A. C.; Sreearunothai, P.; Hertz, L. M.; Friend, R. H.; Silva, C. Exciton regeneration at polymeric semiconductor heterojunctions. *Phys. Rev. Lett.* **2004**, *92*, 247402.

45 Mihailetchi, V. D.; Koster, L. J. A.; Hummelen, J. C.; Blom, P. W. M. Photocurrent generation in polymer—fullerene bulk heterojunctions. *Phys. Rev. Lett.* **2004**, *93*, 216601.

46 Schmidtke, J. P.; Friend, R. H.; Silva, C. Tuning interfacial charge-transfer excitons at polymer—polymer heterojunctions under hydrostatic pressure. *Phys. Rev. Lett.* **2008**, *100*, 157401.

47 Electronic excitations in organic based nanostructures. *Thin Films and Nanostructures*; Bassani, G. F., Agranovich, V. M., Eds.; Academic Press: New York, 2003; Vol. 31.

48 Brédas, J.-L.; Beljonne, D.; Coropceanu, V.; Cornil, J. Charge-transfer and energy-transfer processes in π-conjugated oligomers and polymers: A molecular picture. *Chem. Rev.* **2004**, *104*, 4971–5003.

49 *Electron Transfer in Chemistry*; Balzani, V., Ed.; Wiley-VCH: Weinheim, Germany, 2001.

50 Bixon, M.; Jortner, J. Electron transfer: From isolated molecules to biomolecules. *Adv. Chem. Phys.* **1999**, 106–107.